Thalidomide induces limb defects by preventing angiogenic outgrowth during early limb formation

Christina Therapontos[a,b], Lynda Erskine[b], Erin R. Gardner[c], William D. Figg[d], and Neil Vargesson[a,b,1]

[a]National Heart and Lung Institute, Faculty of Medicine, Imperial College London, Sir Alexander Fleming Building, Exhibition Road, London SW7 2AZ, United Kingdom; [b]School of Medical Sciences, Institute of Medical Sciences, University of Aberdeen, Foresterhill, Aberdeen AB25 2ZD, United Kingdom; [c]Clinical Pharmacology Program, SAIC-Frederick, Inc., National Cancer Institute, Frederick, MD 21702; and [d]Molecular Pharmacology Section, National Cancer Institute, National Institutes of Health, Bethesda, MD 20892

Edited by Clifford J. Tabin, Harvard Medical School, Boston, MA, and approved April 2, 2009 (received for review February 10, 2009)

Thalidomide is a potent teratogen that induces a range of birth defects, most commonly of the developing limbs. The mechanisms underpinning the teratogenic effects of thalidomide are unclear. Here we demonstrate that loss of immature blood vessels is the primary cause of thalidomide-induced teratogenesis and provide an explanation for its action at the cell biological level. Antiangiogenic but not antiinflammatory metabolites/analogues of thalidomide induce chick limb defects. Both in vitro and in vivo, outgrowth and remodeling of more mature blood vessels is blocked temporarily, whereas newly formed, rapidly developing, angiogenic vessels are lost. Such vessel loss occurs upstream of changes in limb morphogenesis and gene expression and, depending on the timing of drug application, results in either embryonic death or developmental defects. These results explain both the timing and relative tissue specificity of thalidomide embryopathy and have significant implications for its use as a therapeutic agent.

blood vessels | chick limb development | thalidomide analog | angiogensis | zebrafish

Half a century ago, thalidomide was used for its antiemetic properties by pregnant women worldwide. It caused an increase in miscarriage and still birth rates and a 40% increase in infant mortality, and up to 10,000 children around the world were born with severe limb malformations, as well as other much less common congenital defects (1–7). Children with such defects are still being born today, particularly in Africa and South America, where thalidomide is now increasingly used in treating leprosy (8, 9). Over 80% of children born to mothers who took thalidomide had limb defects (2, 3, 5, 6). These defects ranged from absence of the limb (amelia) or proximal limb elements (phocomelia) to loss of the thumb or digit tip and are induced in a small time-sensitive developmental window (2, 3, 6–8). The precise mechanism underlying thalidomide's teratogenic effects, its relative limb specificity, and the range of induced defects have not been established.

Thalidomide is both antiinflammatory and antiangiogenic. Its antiangiogenic effects have led to it being postulated as an anticancer agent and are also suggested as being causal in creating limb teratogenesis (1, 8, 10, 11). However, whether the antiangiogenic effect does cause limb defects has neither been confirmed in vivo nor is it known why the limb vasculature would be targeted specifically. Others have proposed that thalidomide affects limb development by inducing changes in gene expression (8, 12–15). Again, neither the mechanism by which thalidomide targets limb gene expression preferentially nor whether such changes are the primary cause of the limb defects has been established. Here we show conclusively that loss of newly formed blood vessels is the primary cause of thalidomide teratogenesis, and developing limbs are particularly susceptible because of their relatively immature, highly angiogenic vessel network. We also demonstrate that these effects correlate to the increased fetal loss and developmental-time-sensitive action of thalidomide (2, 3, 6–8).

Results and Discussion

Antiangiogenic but Not Antiinflammatory Metabolites and Analogues of Thalidomide Induce Limb Defects. Thalidomide applied to HH St17–19 chick embryos, when limbs are beginning to form, induces limb malformations (12, 16, 17) (Fig. S1). However, thalidomide is a very complex molecule, requiring metabolic breakdown to achieve activity and forming potentially over 100 byproducts (1, 18). The major functions of these byproducts are antiinflammatory or antiangiogenic (1, 18). To determine the precise mechanism of thalidomide embryopathy, we have investigated the teratogenic activity of specific thalidomide metabolites and synthesized analogues with distinct biological effects (1, 18–21) (Fig. S2 *A–F*). Drugs were applied over the upper body and amniotic fluid of HH St17–19 embryos, at a similar or lower concentration relative to the therapeutic dose of thalidomide used in humans (chick = 160–1,280 μg/kg; human = 700–2,000 μg/kg). This method of drug application preferentially treats the right limb, allowing us to use the left limb as a control. Antiinflammatory and thalidomide hydrolysis byproducts [5,6-OH thalidomide; 5′OH-thalidomide; PG Acid (*N*-phthaloylglutamic acid)] (18, 21–23) had no effect on embryonic or limb development at any concentration tested [100–800 μg/mL; 160–1,280 μg/kg (n = 16/16 each experiment)] (Fig. S2 *G–J*). However, CPS49, a tetrafluorinated analogue of thalidomide that is chemically and structurally related to thalidomide breakdown products, induced severe limb defects similar to those seen after addition of thalidomide (Fig. 1 *A* and *B* and Figs. S1 and S2*F*) (12, 16, 17). Addition of CPS49 (100 μg/mL; 160 μg/kg), which has potent antiangiogenic and antitumor effects in vitro (18, 20, 21, 24), induced defects in 82% (n = 250/306) of forelimbs and 10% (n = 32/306) of hindlimbs (Fig. 1 *E*, *H*, *J–L*). Defects were not observed in any other regions of the embryo (Fig. 1 *A* and *B*).

Angiogenic Defects Occur Before Changes in Limb Morphology. To determine the effects of CPS49 on the development of the forming limb vasculature, the vascular network was visualized with Indian ink (Fig. 1 *C–H*). Within 2 h of treatment, before obvious changes in limb morphology were observed, CPS49 consistently induced a 20% reduction in vessel density relative to controls (n = 5) (Fig. 1*I*). Vessel density continued to decrease and was reduced by 34% (n = 7) and 45% (n = 12) by 3 h and 6 h posttreatment, respectively, whereas limb area was unaltered or only mildly reduced (Fig. 1 *C*, *D*, *F*, *G*, and *I*). Vessels were regressing visibly by 6 h post CPS49 treatment, resulting in an

Author contributions: N.V. designed research; C.T., E.R.G., and N.V. performed research; W.D.F. contributed new reagents/analytic tools; C.T., L.E., E.R.G., W.D.F., and N.V. analyzed data; and L.E. and N.V. wrote the paper.

The authors declare no conflict of interest.

This article is a PNAS Direct Submission.

[1]To whom correspondence should be addressed. E-mail: n.vargesson@abdn.ac.uk.

This article contains supporting information online at www.pnas.org/cgi/content/full/0901505106/DCSupplemental.

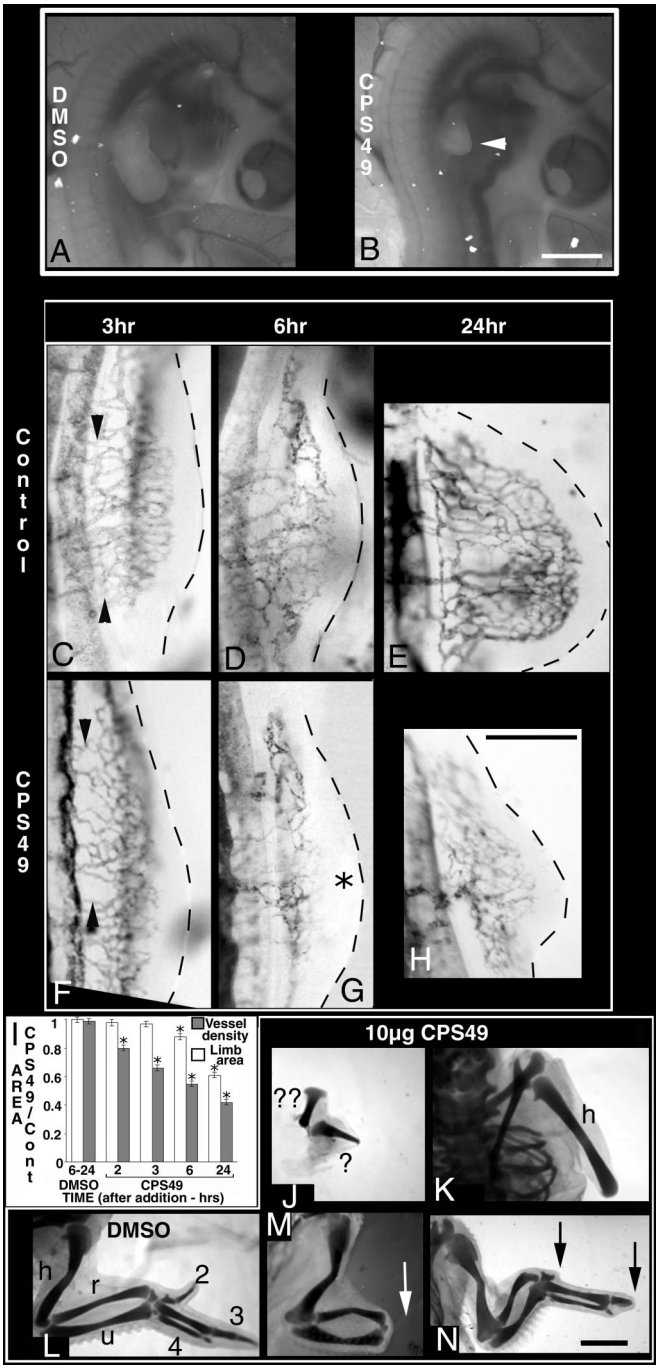

Fig. 1. CPS49 targets limb vasculature and causes limb malformations. (*A*, *B*) Images of living embryos 48 h after treatment at HH St18 with DMSO (*A*) or CPS49 (*B*). With the exception of the forelimb, which is truncated (white arrowhead), the embryo and all blood vessels are normal after CPS49 treatment. (*C–H*) Indian ink injected embryos after treatment with DMSO or CPS49 at HH St18. (*F*) CPS49 inhibits limb vessel angiogenesis within 3 h relative to the DMSO control (*C*, compare arrowheads). By 6 h, in contrast to the DMSO control (*D*) a large avascular zone is present in distal limb tissue (*G*, asterisk), and after 24 h instead of a limb bud with a highly patterned vascular network (*E*), the limb is severely stunted with a markedly reduced vasculature (*H*). (*I*) Mean (± SEM) limb area (open bars) and blood vessel density (filled bars) normalized to the contralateral (untreated) side in control (DMSO) and CPS49 treated limbs. *, $P < 0.01$ compared with control (student's unpaired *t* test). CPS49 treatment induces a rapid decrease in blood vessel density before changes in limb area occur. (*J–N*) Cartilage stains of limbs 10 days after treatment with DMSO (*L*) or CPS49 (*J* and *K*) at HH St18 results in severe limb truncation defects, at HH St24 (*M*) loss of handplate (white arrow), and at HH St28 (*N*) loss of digit tips (black arrows). h, humerus; u, ulna; r, radius; 2, digit2; 3, digit3; 4, digit4; ? and ?? represent 2 severely truncated/shortened articulating cartilage elements. (Scale bars: *A* and *B*, 1,000 μm; *C–H*, 500 μm; *J–N*, 1,750 μm.)

enlarged avascular region in the distal limb bud (Fig. 1 *D* and *G*). By 24 h, vessel density was decreased by 64% and the limb bud itself was severely truncated ($n = 12$) (Fig. 1 *E*, *H*, and *I*). Significantly, other blood vessels and the structure of other tissues in the embryo were unaffected (Fig. 1 *A* and *B*).

Embryos that were viable at day 10 were stained to investigate limb cartilage patterns (Fig. 1 *J–L*). CPS49 treatment resulted in 4 main truncation phenotypes that resemble the range of limb defects seen in thalidomide-affected children: complete forelimb loss (amelia; 21%), a short humerus-like structure (36%; Fig. 1*K*), a shortened humerus with short ulna (21%), or a severely truncated limb with 2 shortened cartilage elements articulating with each other (21%) ($n = 14$) (Fig. 1*J*).

Defects in Vascular Development Occur Upstream of Changes in Cell Death, Proliferation, and Signaling. To determine the sequence of events after CPS49 treatment, we compared the time course of the limb vessel defects with changes in cell death, proliferation, and signaling. Cell death is not detected normally in limb buds until HH St21 and is restricted to specific regions (25). In agreement, at HH St17–19, 3 h post-CPS49 treatment when striking changes in limb vessels have occurred already (Fig. 1 *C* and *F*), cell death was undetectable in the limb (Fig. 2 *A* and *D*). However, cell death was activated in limb-bud mesenchyme by 6 h post-CPS49 treatment (HH St18–20) ($n = 8/8$) (Fig. 2 *B* and *E*), and after 24 h, cell-death-positive cells were present throughout the resulting limb stump (HH St22) ($n = 6/6$) (Fig. 2 *C* and *F*). Cell proliferation also was unaffected at 3 ($n = 3/3$) and 6 h ($n = 6/6$) post-CPS49 treatment (Fig. 2 *Q–S*). Expression patterns of genes essential for limb outgrowth, *Fgf8* in the AER and *Fgf10* in the underlying mesenchyme, were decreased significantly, but not until after changes to blood vessel pattern already had occurred. At 3 h, expression domains of both *Fgf8* and *Fgf10* were identical to control limbs ($n = 5/5$ each) (Fig. 2 *G* and *J*). By 6 h post-CPS49 treatment, *Fgf8* expression was reduced slightly ($n = 3/6$) (Fig. 2*H*), whereas *Fgf10* expression remained normal ($n = 6/6$) (Fig. 2*K*), and by 24 h, expression of both *Fgf8* and *Fgf10* was undetectable in the limbs ($n = 7/7$ each) (Fig. 2 *I* and *L*). In all other regions of the embryo, expression of both genes was unaffected at all time points (Fig. S3 *E* and *F*). Expression of other genes critical for normal limb development either was unaffected or altered, but only after changes in blood vessels already had occurred. Expression of *Bmp4*, involved in apoptosis, was normal until 6 h, but reduced at 24 h (Fig. 2 *M* and *N*). Expression of *HIF-1α*, induced in response to hypoxia, was present at 6 h, but lost within 24 h of treatment suggesting that the ectopic and rapid cell death induced after CPS49 treatment is not caused by hypoxia (Fig. 2 *O* and *P*), but rather a lack of nutrients and build up of waste or toxic products that disrupt the signaling loops between the apical ridge and mesenchyme. Expression of *Tbx5*, required for forelimb initiation ($n = 8/8$), was detectable at all time points (Fig. S3*A*). In contrast, expression of *Shh*, involved in digit patterning ($n = 4/4$), and *Msx1*, a marker of the progress zone, was normal until 6 h, but reduced or undetectable by 24 h ($n = 8/8$ for each) (Fig. S3 *B-D*). Thus, the first detectable change in the developing limb is in blood vessels, with increased apoptosis and disruption of gene expression occurring as a consequence of the effect on the vessels. Our findings strongly suggest that limb blood vessels are targeted directly by CPS49, and is the primary cause of the associated limb defects.

CPS49 Destroys Angiogenic, Immature Vessels, but Not Mature Vessels. Given that development of the entire embryo depends critically on the formation of a normal vascular network (26), why are limbs targeted selectively by CPS49? At the time of drug application, in contrast to vessels throughout the remainder of the embryo, limb vessels are relatively immature, highly angio-

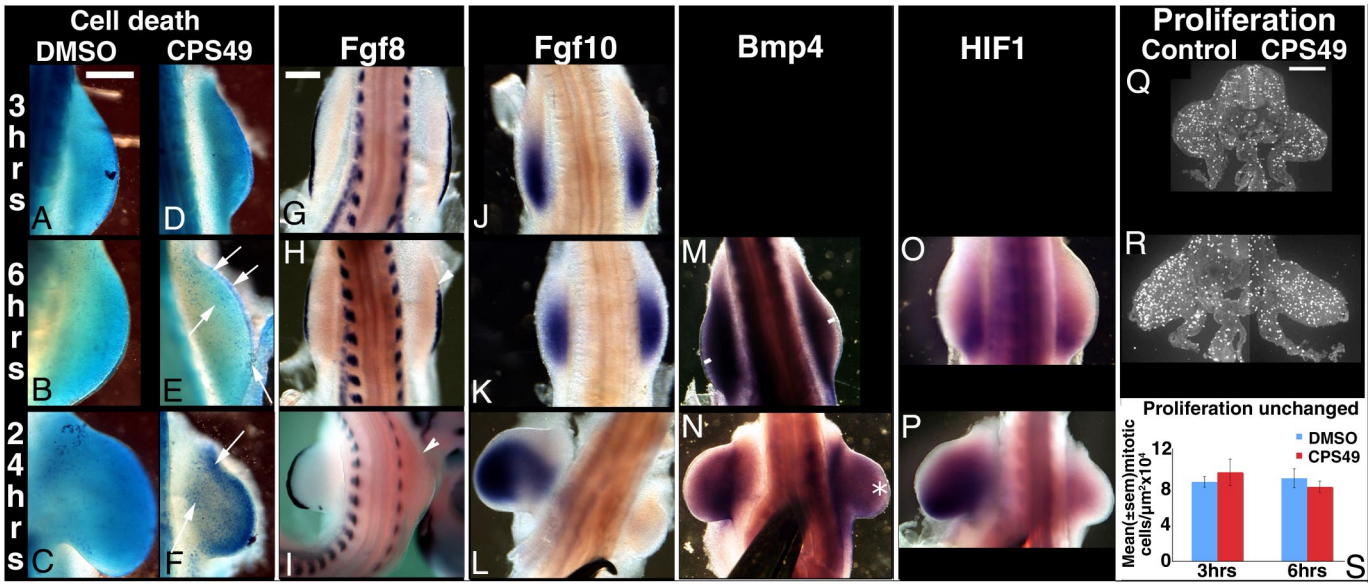

Fig. 2. Changes in limb signaling events occur secondary to vascular inhibition. (*A–P*) HH St18 embryos treated with DMSO or CPS49 and fixed 3 h, 6 h, or 24 h later and stained for cell death (*A–F*) or by wholemount in situ hybridization for *Fgf8* (*G–I*), *Fgf10* (*J–L*), *Bmp4* (*M* and *N*), or *HIF-1* (*O* and *P*) expression; untreated limb to left (*G–P*). (*E* and *F*) Arrows indicate increased cell death in CPS49-treated limbs. (*H* and *I*) Arrowheads indicate decreased *Fgf8* expression relative to the contralateral limb, which serves as an internal control. (*M*) White bars indicate no loss of distal expression of *Bmp4*. (*N*) White asterisk indicates decreased expression of *Bmp4*. (*Q* and *R*) HHst 18 embryos fixed 3 h (*Q*) or 6 h (*R*) after CPS49 treatment and stained with anti-phosphohistone-H^3 to label proliferating cells. Contralateral, untreated limb on left; CPS49-treated limb on right. (*S*) The area of each limb section was calculated by using ImageJ software and the number of proliferating cells determined per unit limb area (μm^2). There is no significant difference in numbers of proliferating cells in CPS49-treated limbs as compared with control limbs. (Scale bars: *A–F*, 500 μm; *G–I*, 400 μm; *Q–S*, 250 μm.)

genic, and lack vascular smooth muscle cells, a marker of maturity (26) (Fig. S4). We used mouse aortic ring cultures to test whether immature and mature blood vessels respond differentially to CPS49 (Fig. 3). CPS49 (10 μg/mL) was added to cultures grown for either 2 or 5 days in vitro (D.I.V.). After 2 D.I.V., cultures contained rapidly growing, immature vessels lacking smooth muscle cells, whereas after 5 D.I.V, vessels were more stable and expressed markers of vessel maturity such as smooth muscle actin (Fig. 3 *A*, *D*, *G*, and *J*). Addition of CPS49 to cultures grown for 2 D.I.V. induced a 57% loss of microvessels within 6 h (Fig. 3 *B*, *C*, and *M* and Table S1). In contrast, CPS49 had no effect on vessel number in cultures grown for 5 D.I.V. (Fig. 3 *H*, *I*, *K*, *L*, and *N* and Table S1), which correlates precisely with the CPS49-induced loss of immature limb vessels (Fig. 1 *F*, *G*, and *I*), but not of more mature vessels throughout the rest of the embryo (Fig. 1 *A* and *B*). However, mature blood vessels are not completely insensitive to CPS49. At both day 2 and 5 D.I.V., outgrowth of surviving blood vessels is inhibited temporarily, resulting in a significant decrease in vessel length by 6 h, followed by partial recovery by 24 h (Fig. 3*O*). This recovery fits with previous reports suggesting CPS49 is active in vitro for 12–18 h (27). Identical results were obtained by using cultures of rat aortic rings (Fig. S5). Together, these results demonstrate directly that CPS49 blocks, temporarily, distal outgrowth from all vessels and, more importantly, kills immature, highly angiogenic but not more mature vessels.

CPS49 Targets the Endothelial Cell Cytoskeleton Preventing Filopodial Outgrowth and Tube Formation. To determine directly the effect of CPS49 on angiogenic outgrowth and sprouting of endothelial cells, we used 2 different approaches. First, we treated transgenic fli1-EGFP transgenic zebrafish embryos (28) with CPS49 (15 μg/mL) and, by using time-lapse imaging, analyzed the development of the intersomitic blood vessels over a 3 h period. CPS49 decreased significantly the number of tip cell filopodia, actin-rich structures essential for endothelial cell migration and outgrowth (Fig. 4 *A–G*). The loss of filopodia was associated with a dramatic decrease in the extent of vessel outgrowth, resulting in failure to establish a normal vascular network (Fig. 4 *A–F* and *H*). Second, we added CPS49 to cultures of cells from a human umbilical vein endothelial cell line (HUVEC). Normally these cells assemble rapidly into tubes highly reminiscent of blood vessels (20). Addition of CPS49 (10 μg/mL) to newly plated HUVEC cells blocked tube formation completely (Fig. 3 *P* and *Q*). Later addition of the drug to cultures in which tubes had already formed did not affect the preexisting tubes, but prevented expansion and growth (Fig. 3 *R–T*). These findings are in striking agreement with our results from the aortic ring cultures (Fig. 3 and Fig. S5), confirming that CPS49 has differential effects on blood vessels depending on their stage of development. At the cellular level, we found that CPS49 induce marked changes in the actin and microtubule cytoskeleton within 1 h (Fig. 4 *I–L*). CPS49 (10 μg/mL) induced the formation of actin stress fibers (Fig. 4 *I* and *K*) and microtubule depolymerization (Fig. 4 *J* and *L*). Such changes are associated with changes in cell migration and proliferation respectively (11). All of these data taken together demonstrate that CPS49 targets the angiogenic endothelial cell actin and microtubule cytoskeleton, resulting in a loss of tip cell filopodia. In newly generated, unstable vessels these changes are associated with complete vessel loss, whereas in more mature, stable vessels, the preexisting vessel is relatively unaffected, but unable, temporarily, to generate new outgrowth (Fig. 4*M*). The effect of CPS49 on tissue development therefore depends on the state of the underlying vasculature. In tissues such as the limb, with rapidly growing and remodeling, immature vessel networks, the CPS49-induced vessel loss results in severe developmental defects. In contrast, in other embryonic regions with more mature, stable vessel networks, the temporary impairment of vessel outgrowth has no significant impact on normal development.

CPS49 Affects Embryonic Development During a Specific Time Window. If our model is true, addition of CPS49 at earlier or later stages of development should result in more or less severe

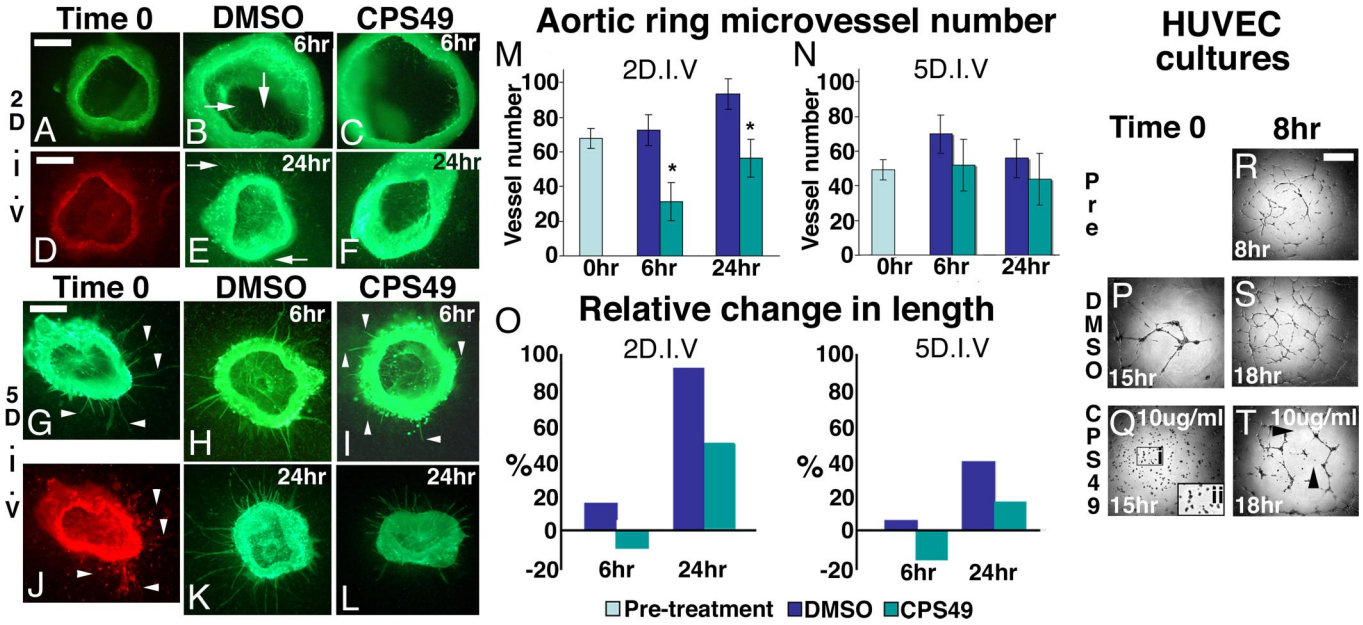

Fig. 3. CPS49 targets angiogenic blood vessels. (*A–L*) Mouse aortic ring cultures at day 2 (*A–F*) and day 5 (*G–L*) stained with IsolectinB4-AlexaFluor488 conjugate to label endothelial cells (*A–C*, *E–I*, *K*, and *L*) or anti-alpha-Smooth muscle actin (*D* and *J*). Vessels in 2 D.I.V. cultures lack smooth muscle (*D*), whereas at 5 D.I.V. smooth muscle is present (*J*; indicated by arrowheads, compare with *G*). Cultures were treated with DMSO (*B*, *H*, *E*, and *K*) or CPS49 (*C*, *F*, *I*, and *L*) and fixed after 6 h (*B*, *C*, *H*, and *I*) or 24 h (*E*, *F*, *K*, and *L*). (*M* and *N*) Mean ± SEM microvessel count of day 2 and day 5 cultures. CPS49 induces a significant decrease in microvessel number from 2 D.I.V. (compare *C* and *F* with *B* and *E*; arrows highlight vessels) but not 5 D.I.V. cultures (compare *H* and *I*; arrowheads indicate vessels). (*O*) Percentage change in surviving vessel after addition of CPS49. In both 2 D.I.V. and 5 D.I.V., surviving vessels retract initially after CPS49 treatment, resulting in a decrease in vessel length 6 h posttreatment. Outgrowth resumes subsequently, but by 24 h posttreatment vessels are still stunted compared with controls. (*P–T*) Cultures of HUVEC cells treated with DMSO (*P* and *S*) or 10 μg/mL CPS49 (*Q* and *T*). Addition of CPS49 at the time of plating prevented vascular tube formation (*P* and *Q*). (*Q*) Boxed area *i* is enlarged (*ii*), indicating no connections or tube formations between HUVEC cells, whereas addition after 8 h in culture, when a vascular network has formed already (*R*), had no impact on preexisting vessel tubes but prevented further elaboration of the network (*S* and *T*). ⋆, $P < 0.01$ compared with control (Student's unpaired *t* test). (Scale bars: *A–C*, 200 μm; *D–L*, 400 μm; *R–T*, 300 μm.)

defects, respectively. Our findings confirm our model and correlates with the time-sensitive period of thalidomide action in human pregnancy (1–5). Application of CPS49 to HHst13–15 embryos (day 2) when the embryo is just beginning to be vascularized, with highly angiogenic, immature vessels, results in 100% embryonic lethality within 12 h (n = 12/12) (Fig. S6). Conversely, addition at later stages (HHst24–28) generated progressively less-severe limb defects. At HHst24, CPS49 induced loss of only the handplate (n = 6/6) (Fig. 1*M*) as opposed to the majority of limb structures after addition at HHst17 (Fig. 1 *J* and *K*). At HHst28, the effects were even less severe with only the tips of digits 2 and 3 lost (n = 6/6/) (Fig. 1*N*).

Conclusions

A large number of models and hypotheses have been previously published that try to explain the basis of thalidomide-induced limb defects (8, 12–15). Such models include changes in gene expression (8, 12–15), induction of oxidative stress (8, 14, 15), effects on chrondrogenesis (8), mutation of DNA (8), limb bud distalization (13), and induction of cell death (8, 12). These models, although interesting, do not address how thalidomide targets the limb preferentially. Our data clearly demonstrate that the primary cause of thalidomide-induced limb malformations is the loss of the forming limb vasculature. As a consequence, changes in cell death and loss of gene signaling pathways then result. A challenge for the future will be to determine the sequence of cell and molecular changes after vascular inhibition in the limb. Thalidomide can also induce other defects to the body, notably to the ears, eyes, heart, kidney, and genitals (1–8). Whether these defects also are caused by preventing angiogenesis, in a time-sensitive manner as these forming tissues are being vascularized, remains to be established and is the focus of ongoing work. A surprising feature of thalidomide is that it is not teratogenic in some animal species, particularly the mouse (2, 8, 29). However, our results clearly show that mouse blood vessels are sensitive to CPS49 (Fig. 3). One possibility is that thalidomide does not pass through the mouse placenta. Alternatively, the antiangiogenic products, related to CPS49, are not generated in these species. Indeed, previous work has demonstrated that the metabolic activation of thalidomide is species dependent (30). Further studies will be required to test these models.

By using CPS49, a bioactive analogue of thalidomide that is related to thalidomide breakdown products, we have resolved a 50-year-old puzzle and demonstrated, by using a range of in vivo and in vitro systems, that differential effects on immature and more stable blood vessel networks explains the thalidomide embryopathy seen in humans. Furthermore, we describe the basis of CPS49 action on the endothelial cell, showing that filopodial outgrowth is inhibited and cells are prevented from proliferating and migrating and from forming vascular tubes providing an explanation for its effects at the cellular level. Our results explain the increased fetal loss, the range of developmental abnormalities, and even the time-sensitive window of the drug, all dependent on the state of the vasculature at the time of drug application. Furthermore, we show that in the developing limb, thalidomide/CPS49-induced vessel loss is the primary trigger leading to increased cell death and impairment in limb signaling pathways, resulting consequently in limb outgrowth failure and truncations (Fig. 4*N*). A remaining puzzle is the mechanism by which phocomelia (loss of proximal but not distal elements) occurs. An intriguing possibility for how this arises in humans is that in some instances a partial loss of FGF signaling is induced because in mice this results in loss of proximal limb elements (31) (Fig. 4*N*). Such an effect could occur through

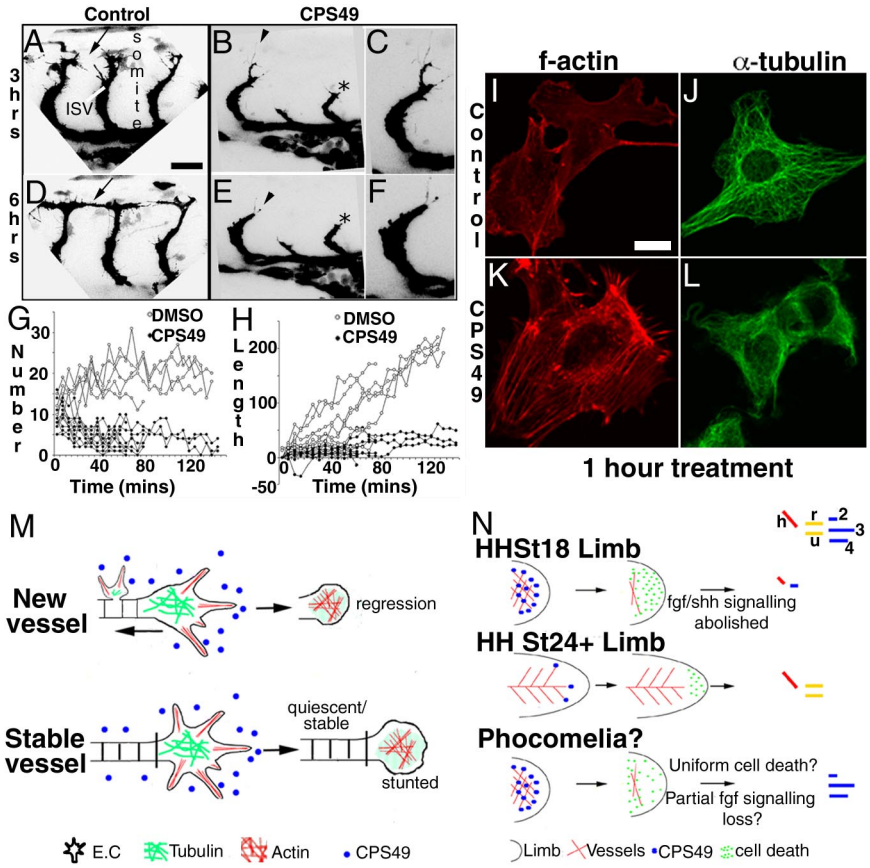

Fig. 4. CPS49 prevents filopodial extensions in endothelial cells. (*A–F*) Confocal images of zebrafish intersomitic vessel (ISV) formation 3 h (*A–C*) or 6 h (*D–F*) after DMSO (*A* and *D*) or CPS49 (*B*, *C*, *E*, and *F*) treatment at 24 h postfertilization. Black arrowheads in *B* and *E* are shown at higher power in *C* and *F*. CPS49 reduced the number of filopodia and filopodial extensions (arrowheads), stunted forming ISVs (black asterisk), and prevented formation of a patent, functional vascular network (black arrows; compare *A*, *B*, *D*, and *E*). (*G* and *H*) Number of tip cell filopodia (*G*) and accumulative change in ISV length (*H*) in control (DMSO; open circles) and CPS49 (filled circles) treated zebrafish embryos imaged by using time-lapse photography. (*I–L*) Confocal images of HUVEC cultured cells after 1 h of treatment with DMSO (*I* and *J*) or CPS49 (*K* and *L*). f-actin antibody staining highlights increased stress fibers in CPS49-treated cells (*K*) but not in DMSO-treated cells (*I*). alpha-tubulin staining indicates a decrease in tubulin structure between DMSO (*J*) and CPS49 (*L*) treated cells. (*M*) Model of CPS49 action on endothelial cell and vessel outgrowth, where new vessel networks are stunted and lost as CPS49 prevents all angiogenesis, but in stable, established, mature networks, only the distal cell is prevented from angiogenesis and stunted temporarily. (*N*) Model of action of CPS49 of the limb highlighting the developmental stage dependence of drug action. Treatment at HHst18 results in limb outgrowth failure, as all vessels are unstable and affected, whereas at HHst23, proximal vessels are stable, but distal vessels are angiogenic and lost resulting in loss of the handplate. We hypothesize that phocomelia arises because of some FGF signaling remaining, which can then pattern the resulting limb stump. (Scale bars: *A*, *B*, *D*, and *E*, 25 μm; *C* and *F*, 12.5 μm; *I–L*, 10 μm.)

diffuse, widespread mesenchymal cell death, leaving some FGF signaling function in the apical ridge, in turn allowing the FGFs to distalise the resulting limb stump, after the drug action has worn off (Fig. 4*N*).

By demonstrating that CPS49 differentially affects blood vessels depending on their state of maturity, this work will impact significantly on the development of thalidomide/CPS49 as a treatment for early stage cancer, as well as production of a nonteratogenic version of thalidomide retaining the therapeutic benefits. This work also provides a platform to study the development and origins of other limb malformations, one of the most common birth defects in humans (32).

Materials and Methods

Chick Embryology and Analysis. White Leghorn chick eggs (provided by Henry Stewart, Lincolnshire, United Kingdom) were incubated at 37° C until the required developmental stage (33) and until the membranes were removed for drug application to the embryo. Thalidomide analogues and metabolites were dissolved in DMSO (Sigma) at concentrations of 40 mg/mL and were diluted in prewarmed DMEM (Sigma Aldrich) to 100 μg/mL (CPS49) or 100–800 μg/mL (5,6-OH thalidomide, 5′OH-thalidomide, PG Acid). Drugs (100 μL) or vehicle alone (0.1% DMSO) (Sigma Aldrich) were applied to the upper half of the embryo, which lies on its left side and, because of limited diffusion of drugs, this side was normal after treatment and acted as an internal control. Embryos were fixed overnight in 4% paraformaldehyde in PBS for wholemount in situ hybridization, 5% trichloroacetic acid for cartilage staining, or Dents fixative for wholemount antibody staining.

For cartilage staining, embryos were rinsed in 70% ethanol, stained in 0.1% alcian blue/1% hydrochloric acid/70% ethanol for 6 h, rinsed overnight in acid-ethanol, dehydrated, and cleared in methyl salicyclate. Wholemount in situ hybridization or antibody staining was performed as detailed previously (26). Anti-alpha-Smooth muscle actin (1A4) (Sigma) was used at 1:1,000, antiphosphohistone H3 (Millipore) at 1:100, and AlexaFluor 568 (Invitrogen) at 1:1,500. Ink injections to label the vasculature were carried out as described previously (26). Blood vessel density was measured by using ImageJ software to count the number of pixels covered by the vascular network and normalized to the contralateral control. Cell death was visualized by placing embryos with their membranes removed into a 1 mg/mL solution of Nile Blue Sulfate (Sigma Aldrich) dissolved in water and filtered. Embryos were left at 37° C for 30 min and placed in fresh PBS.

Analysis and photography were performed by using a Nikon SMZ1500 fluorescent stereomicroscope with a Nikon DS-5 digital camera. Images were prepared by using Adobe Photoshop.

Mouse Aortic Ring Assay. Cultures were prepared based on the rat aortic ring thin-prep assay (34). Briefly, aortic rings were obtained by cross-sectioning the aorta at 1-mm intervals, rinsed in DMEM, and placed on ice in fresh medium.

Collagen solution (1.5 mg/mL) was prepared on ice, by mixing: 1 volume (vol) 10x MEM (Invitrogen), 1.5 vol 15.6 mg/mL $NaHCO_3$, 0.1 vol 1 M NaOH, and 7.5 vol 2 mg/mL rat tail collagen, type I (BD Biosciences). Fifteen microliters of collagen solution were aliquoted in the center of sterile 13-mm glass coverslips, forming a thin disk of 6–7 mm in diameter. After 15–20 min at 37° C, an aortic ring was transferred to each collagen bubble and covered with a further 15 μL of collagen solution. Rings were orientated so that the luminal axis of each ring was lying parallel to the bottom of the dish. After incubation of 15–20 min, each coverslip was transferred to a well in a 24-well plate and 750 μL to 1 mL of endothelial growth medium supplemented with the EGM-2 BulletKit (hydrocortisone, hFGF-B, 2 mL; VEGF, 0.5 mL; R3-IGF-1, 0.5 mL Abscorbic Acid, 0.5 mL; Heparin, 0.5 mL; FBS, 10 mL; hEGF, 0.5 mL; GA-1,000, 0.5 mL) (EGM-2) was added per well. Cultures were incubated at 37° C in a humidified CO_2 incubator with medium change every other day. The day of aortic ring preparation was taken as day 0 of culture. Mouse aortic rings were treated with 10 μg/mL CPS49 or vehicle (0.1% DMSO) on day 2 or day 5 of culture. CPS49 and vehicle were prepared in prewarmed EGM-2, added to the cultures, and incubated for 6 or 24 h. At the end of each incubation, cultures were fixed and stained with the *Griffonia simplicifolia* isolectin-B4, AlexaFluor 488 conjugate (Molecular Probes #I21411) to label endothelial cells and anti-Alpha smooth muscle actin antibody (clone 1A4, mouse monoclonal) (Sigma Aldrich #A2547) to label smooth muscle cells.

Zebrafish Embryology and Time-Lapse Imaging. Fli1-EGFP fish were obtained from the Zebrafish International Resource Center (28). Embryos at 24 h were dechorionated and treated with 15 μg/mL CPS49 or 0.5% DMSO in aquarium medium. After 3 h, embryos were anesthetized with 0.05% MS222 (Tricaine) (Sigma Aldrich) and embedded in 0.5% agarose covered in tricaine. Live visualization of blood vessels was carried out on a Leica TCS-NT laser-scanning confocal microscope. Images were captured every 5 min at $\times$63 magnification at 2.5-μm intervals and processed by using Adobe Photoshop. Measurements of vessel length and filopodia number were performed by using Image J.

HUVEC Endothelial Cell Culture. HUVEC (Lonza #C2517) were cultured in EGM-2 medium with full growth supplements (Lonza). Cells were thawed, maintained, and subcultured according to the supplier's instructions. The Chemicon In Vitro Angiogenesis Assay Kit (#ECM625) was used to evaluate tube formation by endothelial cells in response to CPS49 treatment. The cell cultures were exposed to increasing concentrations of CPS49 (0, 0.1, 1, 10 or 40 μg/mL). The cells were incubated for 18 h at 37° C before being analyzed and photographed for formation of vascular tubes. Pictures of live cells were taken on an Olympus CKX41 inverted cell culture microscope fitted with an Olympus U-CMAD3 camera with ColorView Soft Imaging system. Images were processed and organized in Adobe Photoshop.

Cell Proliferation Analysis. After drug treatment, embryos were dissected in PBS and fixed in 4% PFA overnight at 4° C. Embryos were then placed in 30% sucrose solution in PBS overnight and subsequently embedded in Cryo M Bed (Bright) for cryosectioning. Blocks were frozen by using dry ice and stored at −20° C for up to 1 week. Ten-micrometer sections were cut on a cryostat, allowed to air dry, and stored at −20° C before staining to reveal mitotic cells. The tissue sections were blocked in 10% goat serum in 0.2% Triton X-100 PBS for 90 min at room temperature, before incubation in primary antibody {anti-phospho-histone H3 [Ser-10, rabbit polyclonal IgG (Upstate)] diluted 1:100 in block solution} overnight at 4° C. The following day, the slides were washed several times in PBS and incubated in secondary antibody [goat-anti-rabbit-Cy3 diluted 1:500 in 1% goat serum/PBS] for 2 h at room temperature and in the dark. At the end of the incubation, the slides were washed in PBS, mounted in Vectashield mounting medium for fluorescence (Vector Laboratories), and analyzed by fluorescent microscopy. The number of fluorescent cells were counted per limb bud in each section. The area of each limb was then calculated by using ImageJ software, and the number of proliferating cells was finally determined per unit limb area.

ACKNOWLEDGMENTS. We thank Colin McCaig for comments on the manuscript; Grahame Nixon and Alix McDowell for advice on the mouse aortic ring; Matthew L. Danish and Haihao Sun for technical help on the rat aortic ring; and Elizabeth Kilby and Caroline Lim for technical support with Fig. S1. C.T. was an Imperial College London funded PhD student. This work was funded by grants from the Royal Society and University of London Central Research Fund (to N.V.) and federal funds from the National Cancer Institute, National Institutes of Health, under contract N01-CO-12400 (E.R.G.) and was supported in part by the Intramural Research Program of the National Institutes of Health, National Cancer Institute, Center for Cancer Research (E.R.G. and W.D.F.).

1. Franks ME, MacPherson GR, Figg WD (2004) Thalidomide. *Lancet* 363:1802–1811.
2. Lenz WA (1988) A short history of thalidomide embryopathy. *Teratology* 38:203–215.
3. Lenz W, Knapp K (1962) Foetal malformations due to thalidomide. *Ger Med Mthly* 7:253–258.
4. McBride WB (1961) Thalidomide and congenital abnormalities. *Lancet* 2:1358.
5. Smithells RW (1973) Defects and disabilities of thalidomide children. *BMJ* 1:269–272.
6. Smithells RW, Newman CGH (1992) Recognition of thalidomide defects. *J Med Genet* 29:716–723.
7. Matthews SJM, McCoy S (2003) Thalidomide: A review of approved and investigational uses. *Clinical Therapeutics* 25:342–395.
8. Stephens TD, Bunde CJW, Fillmore BJ (2000) Mechanism of action in thalidomide teratogenesis. *Biochem Pharm* 59:1489–1499.
9. Schuler-Fuccini, et al. (2007) New cases of thalidomide embryopathy in Brazil. *Birth Defects Res (Part A)* 79:671–672.
10. D'Amato RJ, Loughnan MS, Flynn E, Folkman J (1994) Thalidomide is an inhibitor of angiogenesis. *Proc Natl Acad Sci* 91:4082–4085.
11. Tamilarasan KP, et al. (2006) Thalidomide attenuates nitric oxide mediated angiogenesis by blocking migration of endothelial cells. *BMC Cell Biology* 7:17.
12. Knobloch J, Shaughnessy JD, Jr, Ruther U (2007) Thalidomide induces limb deformities by perturbing the Bmp/Dkk1/Wnt signalling pathway. *FASEB J* 21:1410–1421.
13. Tabin CJ (1998) A developmental model for thalidomide defects. *Nature* 396:322–323.
14. Knobloch J, Reimann K, Klotz LO, Ruther U (2008) Thalidomide resistance is based on the capacity of the glutathione-dependent antioxidant defense. *Mol Pharmaceutics* 5:1138–1144.
15. Hansen JM, Harris C (2004) A novel hypothesis for thalidomide-induced limb teratogenesis: Redox misregulation of the NF-kappaB pathway. *Antioxid Redox Signal* 6:1–14.
16. Boylen JB, Horne HH, Johnson WJ (1963) Teratogenic effects of thalidomide and related substances. *Lancet* 1:552.
17. Jurand A (1966) Early changes in limb buds of chick embryos after thalidomide treatment. *J Embryol Exp Morphol* 16:289–300.
18. Lepper ER, Smith NF, Cox MC, Scripture CD, Figg WD (2006) Thalidomide metabolism and hydrolysis: Mechanisms and implications. *Curr Drug Metab* 7:677–685.
19. Lepper ER, et al. (2004) Comparative molecular field analysis and comparative molecular similarity indices analysis of thalidomide analogues as angiogenesis inhibitors. *J Med Chem* 47:2219–2227.
20. Ng SSW, et al. (2003) Antiangiogenic activity of N-substituted and tetrafluorinated thalidomide analogues. *Cancer Res* 63:3189–3194.
21. Ng SS, MacPherson GR, Gutschow M, Eger K, Figg WD (2004) Antitumor effects of thalidomide analogs in human prostate cancer xenografts implanted in immunodeficient mice. *Clin Cancer Res* 10:4192–4197.
22. Nakamura T, Noguchi T, Kobayashi H, Miyachi H, Hashimoto Y (2006) Mono- and dihydroxylated metabolites of thalidomide: Synthesis and TNF-alpha production-inhibitory activity. *Chem Pharm Bull* 54:1709–1714.
23. Nakamura T, Noguchi T, Miyachi H, Hashimoto Y (2007) Hydrolyzed metabolites of thalidomide: Synthesis and TNF-alpha production-inhibitory activity. *Chem Pharm Bull* 55:651–654.
24. Warfel NA, Lepper ER, Zhang C, Figg WD, Dennis PA (2006) Importance of the stress kinase p38 in mediating the direct cytotoxic effects of the thalidomide analogue, CPS49, in cancer cells and endothelial cells. *Clin Cancer Res* 12:3502–3509.
25. Fernandez-Teran MA, Hinchliffe JR, Ros MA (2006) Birth and death of cells in limb development: A mapping study. *Dev Dynamics* 235:2521–2537.
26. Vargesson N, Laufer E (2001) Smad7 misexpression during embryonic angiogenesis causes vascular dilation and malformations independently of vascular smooth muscle cell function. *Dev Biol* 240:499–516.
27. Kumar S, et al. (2005) Antimyeloma activity of two novel N-substituted and tetrafluorinated thalidomide analogs. *Leukemia* 19:1253–1261.
28. Lawson ND, Weinstein BM (2002) In vivo imaging of embryonic vascular development using transgenic zebrafish. *Dev Biol* 248:307–318.
29. Stephens TD, Fillmore BJ (2000) Hypothesis: Thalidomide embryopathy – Proposed mechanism of action. *Teratology* 61:189–195.
30. Bauer KS, Dixon SC, Figg WD (1998) Inhibition of angiogenesis by thalidomide requires metabolic activation, which is species-dependent. *Biochem Pharmacol* 55:1827–1834.
31. Mariani FV, Ahn CP, Martin GR (2008) Genetic evidence that FGFs have an instructive role in limb proximal-distal patterning. *Nature* 453:401–405.
32. Wilkie AOM (2002) Why study human limb malformations? *J Anat* 202:27–35.
33. Hamburger V, Hamilton HL (1951) A series of normal stages in the development of the chick embryo. *J Exp Morphol* 88:49–92.
34. Zhu W-H, Nicosia RF (2002) The thin prep rat aortic ring assay: A modified method for the characterization of angiogenesis in whole mounts. *Angiogenesis* 5:81–86.